
LNL+K: Learning with Noisy Labels and Noise Source Distribution Knowledge

Siqi Wang
Boston University
siqiwang@bu.edu

Bryan A. Plummer
Boston University
bplum@bu.edu

Abstract

Learning with noisy labels (LNL) is challenging as the model tends to memorize noisy labels, which can lead to overfitting. Many LNL methods detect clean samples by maximizing the similarity between samples in each category, which does not make any assumptions about likely noise sources. However, we often have some knowledge about the potential source(s) of noisy labels. For example, an image mislabeled as a cheetah is more likely a leopard than a hippopotamus due to their visual similarity. Thus, we introduce a new task called Learning with Noisy Labels and noise source distribution Knowledge (LNL+K), which assumes we have some knowledge about likely source(s) of label noise that we can take advantage of. By making this presumption, methods are better equipped to distinguish hard negatives between categories from label noise. In addition, this enables us to explore datasets where the noise may represent the majority of samples, a setting that breaks a critical premise of most methods developed for the LNL task. We explore several baseline LNL+K approaches that integrate noise source knowledge into state-of-the-art LNL methods across three diverse datasets and three types of noise, where we report a 5-15% boost in performance compared with the unadapted methods. Critically, we find that LNL methods do not generalize well in every setting, highlighting the importance of directly exploring our LNL+K task.¹

1 Introduction

High-quality labeled data is beneficial to deep neural networks (DNNs) training. However, obtaining such datasets is expensive and labels are often corrupted in large real-world datasets [1, 2]. Thus, Learning with Noisy Labels (LNL) [3] has become an important topic in the robust training. The goal of LNL is to effectively learn the feature distribution from the noisy training set and perform well on the clean test set [4, 5]. To avoid overfitting to noisy labels, an ideal model would identify three types of clean samples: easy positives that match the estimated categorical distribution perfectly; hard negatives [6, 7] that are near the decision boundary, and outliers [8] of the estimated distribution but still be representative of the true class. As shown in Fig. 1-a, existing methods [8–16] detect clean samples by finding the most similar samples within each class. Samples that match the category distribution well can be detected this way, while those near the decision boundary and outliers are still challenging. Moreover, a high noise ratio can lead to ambiguity in the estimated distribution, *i.e.*, the noise distribution is estimated instead of its category. For example, the red category in Fig. 1-a has 50% noise, which skews the distribution of the class and ends up selecting the noisy samples.

Our key observation is that prior work does not consider the distribution of noise, which can be beneficial information in LNL for the above-mentioned challenges. Notably, the noise source knowledge is not entirely unknown in real-world datasets. Labels are rarely uniformly corrupted

¹Code available at https://github.com/SunnySiqi/LNL_K

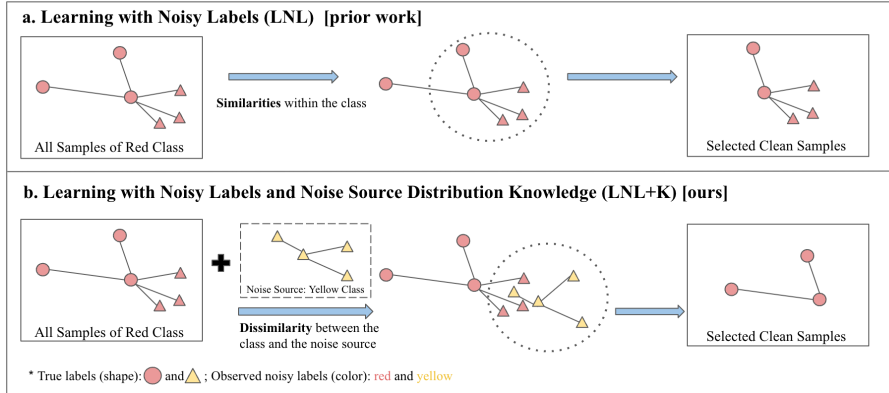


Figure 1: (Best view in color.) **Comparison of a prior work on LNL and our LNL+K task.** **a:** LNL methods [8–16] select clean samples according to the similarity within the same class, while **b:** LNL+K identify clean samples that are least similar to the noise source. This illustrates a failure case of LNL methods when the noise ratio is high, but where an LNL+K approach can succeed.

across all classes, and some classes are more easily to be confused than others [17]. For example, visually similar objects are often mislabeled: *e.g.* knitwear and sweater [18], automobiles and trucks [19]. What’s more, some categories are designed to establish causality in scientific settings and can be treated as noise sources in the training, such as the "control" group [20], *i.e.*, "doing-nothing" group and when no experimental effect happens, the test object should look like "control." Hence, for datasets with such noise source distribution knowledge, exploring how to incorporate knowledge into the clean sample detection process has great potential.

To this end, we introduce a **new task: Learning with Noisy Labels and noise source distribution Knowledge (LNL+K)**. In contrast to traditional LNL tasks, we assume that we are given some knowledge about noisy label distribution. *i.e.*, noisy labels tend to originate from specific categories. For example, the knowledge in Fig. 1 is that the noisy samples are from the yellow class. Compared with LNL that the probability of a sample being clean only depends on the distribution of its labeled class features, LNL+K also takes the distribution of its noise source features into account.

The benefits of integrating noise source distribution knowledge are twofold. First, this knowledge is helpful in distinguishing noisy samples with similar features. Consider the red class in Fig. 1-b, even the noisy red triangles have similar features to the true circle class, given the noise source yellow class, it’s obvious that those noisy samples are closer to their true label class. Second, knowledge is necessary when the noise ratio is high and noisy samples dominate the class distribution. Without knowledge, LNL methods select samples that maximize the similarity within the group, which ends up selecting the noisy ones that dominate the distribution. Unlike most LNL methods that assume an upper bound on the noise ratio [21], LNL+K moves beyond this limitation. Rather than detecting clean-label samples according to how "similar" to other samples in its own class, LNL+K focuses on how "dissimilar" with samples in the noise source class.

In order to demonstrate the benefits of LNL+K methods as mentioned above, we explore several baseline methods of LNL+K by adding noise source distribution knowledge to unsupervised state-of-art LNL methods [9, 10, 22]. The adaptations are made based on a unified framework of clean sample detection in LNL+K. Each adaptation method uses the same feature for clean sample detection as the LNL methods but then also compares the (noisy) class features with the noise source features. Experiments are on both synthesized and real-world datasets with three types of noise, one of which is the dominant noise - a new noise setting we introduce to simulate the high-noise-ratio scenarios where the noisy samples may dominate the class distribution. Results show that adaptation methods outperform the original ones, and rankings change among the methods proves that unsupervised methods have different "knowledge absorption" to the added supervision, *i.e.*, The degree of performance improvements varies for unsupervised LNL methods. These differences in "knowledge absorption" rates indicate that LNL+K is a new task worthy of the research community’s attention.

In summary, our contributions are:

- We introduce a novel task, termed **LNL+K: Learning with Noisy Label and noise source distribution Knowledge**. We also design a new noise setting: dominant noise, where noisy samples are the majority of a labeled category distribution.
- We define a unified framework for clean label detection in LNL+K, and explore three baseline methods for LNL+K by adapting LNL methods with noise source knowledge.
- Our experiments report a 4.5% increase in accuracy with asymmetric noise on synthesized datasets using CIFAR-10/CIFAR-100 [19], with up to a 15% gain on dominant noise. We also obtain a 1.5% accuracy gain on BBBC036 [23], in a real-world noisy dataset for image-based cell profiling [24].

2 Related Work

Hindering the memorization of noisy labels plays a vital role in LNL [25–27]. In order to achieve this objective, different approaches are pursued to detecting noisy labels and robust training.

For clean and noisy sample detection, there are mainly loss-based [28–30] methods that detect noisy samples with high losses, and probability-distribution-based [15, 31–34] approaches that select clean samples with high probability differences between the predicted classes, under the assumption that clean-label samples have high confidence in the prediction. However, these assumptions may not always hold true, especially with hard negative and hard positive samples. Samples selected by these approaches are more likely to be "easy" samples instead of "clean" samples. To retain those boundary samples, Self-Filtering (SFT) [22] observed that noisy samples more easily occur fluctuation, where a sample classified correctly before is misclassified in the later process. Feature-based approaches [9, 10] have also been proposed that utilize the input before the softmax layer – high-dimensional features, which are less affected by noisy labels [35–37]. CRUST [10] uses the Jacobian spectrum of typical neural network gradient descent, which can be split into information space and nuisance space. Finding data points that span the information space can avoid gradient descent to overfit noisy labels. FINE [9] uses the eigenvector of the feature for each class to maximize the alignment values of clean data.

For robust learning, there are methods adjusting the loss function [12, 38–41], using regularization techniques [42–44], and multi-round learning only with selected clean samples [45–47]. LNL+K focuses on exploring noise source distribution knowledge used in the clean sample detection process.

In summary, there are two assumptions underlying LNL methods: 1. Most samples in a class are clean. Even in high noise ratio settings, the noisy samples are from multiple classes, so the category with the most samples is the true label. 2. Noisy samples are very dissimilar to clean ones. Our work demonstrates that noise source distribution knowledge is the key to moving beyond these limitations.

3 Learning with Noisy Labels + Knowledge (LNL+K)

Learning with Noisy Label Source Knowledge (LNL+K) aims to find the optimal parameters set θ^* for the classifier f_θ , which is trained on the noisy dataset D **with noise source knowledge** D_{ns} and achieve high accuracy performance on the clean test dataset. In this section, we first introduce the notation we will use, then we will define a unified clean-sample-detection framework in Section 3.1.

Suppose we have a dataset $D = \{(x_i, y_i)_{i=1}^n \in R^d \times K\}$, where $K = \{1, 2, \dots, k\}$ is the categorical label for k classes. (x_i, y_i) denotes the i -th example in the dataset, such that x_i is a d -dimensional input in R^d and y_i is the label. $\{y_i\}_{i=1}^n$ might include noisy labels and we have no knowledge of the true labels $\{\tilde{y}_i\}_{i=1}^n$. However, we do have some prior knowledge about noisy label sources. The noisy source estimation can be obtained by analysis on a smaller clean subset $D' \subset D$, where $\forall (x_i, y_i) \in D', y_i = \tilde{y}_i$. Therefore, the noise source distribution knowledge D_{ns} can be represented by a probability matrix $P_{k \times k}$, where P_{ij} refers to the probability that a sample in class i is mislabeled as class j . The noise source knowledge can also be summarized with human visual understanding: *e.g.*, automobiles and trucks are visually similar classes and are more likely mislabeled with each other. In this case, the source knowledge can be represented by a set of label pairs $LP = \{(i, j) | i, j \in K\}$, where (i, j) refers to the fact that samples in class i are more likely to be mislabeled as class j . For the convenience of formulating the following equations, D_{c-ns} represents the set of noise source labels of category c . *I.e.*, $D_{c-ns} = \{i | i \in K \wedge (P_{ic} > 0 \vee (i, c) \in LP)\}$.

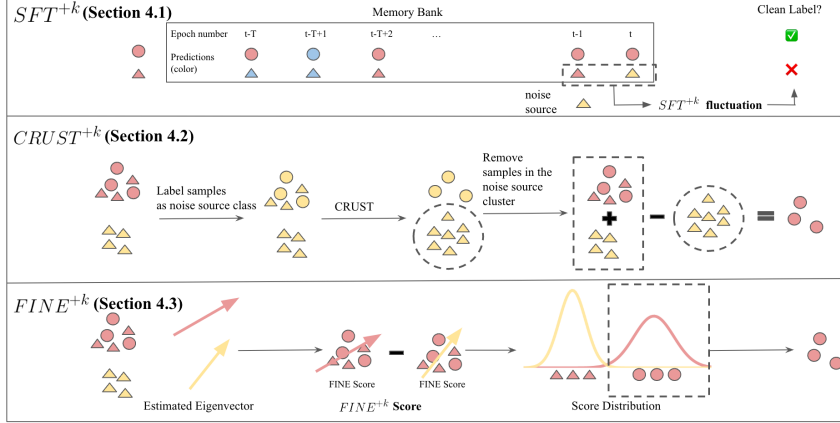


Figure 2: (Best view in color.) **Illustration of LNL+K baseline methods.** SFT^{+k} is adapted by restricting the misclassification in fluctuations only to noise source labels. $CRUST^{+k}$ adaptation is mixing samples with noise source category samples together and removing samples in the noise source cluster. $FINE^{+k}$ is adapted by comparing the class alignment(FINE-score) with noise source class alignment. Details of each adaptation method can be found in the corresponding subsections.

3.1 A Unified Framework for Clean Sample Detection with LNL+K.

To make our framework general enough to represent different LNL methods, we define a unified logic of clean sample detection. In other words, this section provides a general overview of LNL+K methods and summarizes them using a unified set of abstract functions. Section 4 delves into specific adaptation of LNL methods using our framework to use as our baselines.

For LNL methods, sample x_i has a clean categorical label c , *i.e.*,

$$\tilde{y}_i = c \leftrightarrow y_i = c \wedge p(c|x_i) > \delta, \quad (1)$$

where $p(c|x_i)$ is the probability of sample x_i with label c and δ is the threshold for the decision. Different methods vary in how they obtain $p(c|x_i)$. For example, as mentioned in related work, loss-based detection uses $Loss(f_\theta(x_i), y_i)$ to estimate $p(c|x_i)$, probability-distribution-based methods use the logits or classification probability score $f_\theta(x_i)$, and feature-based method use $p(c|x_i) = M(x_i, \phi_c)$, where M is a similarity metric and $\phi_c = D(g(X_c))$ is the distribution of features labeled as category c , *i.e.*, $X_c = \{x_i|y_i = c\}$, $g(X_c) = \{g(x_i, c)|x_i \in X_c\} \sim \phi_c$, and $g(\cdot)$ is a feature mapping function. The feature-based methods often vary in how they implement their feature mapping $g(\cdot)$ function and similarity distance metric M .

LNL+K adds knowledge D_{ns} by comparing $p(c|x_i)$ with $p(c_n|x_i)$, where c_n is the noise source label. When category c has multiple noise source labels, $p(c|x_i)$ should be greater than any of these. In other words, the probability of sample x_i has label c (*i.e.*, $p(c|x_i)$), not only depends on its own value but is decided by the comparison to the noise source labels. For example, the red triangle x_i in Fig. 1 has a high probability of belonging to the red class, *i.e.*, $p(red|x_i) > \delta$, then it is detected as a clean sample in LNL. However, compared to the probability of belonging to the noise source yellow class, $p(yellow|x_i) > p(red|x_i)$, so the red triangle is detected as a noisy sample in LNL+K. To summarize, the propositional logic of LNL+K is:

$$\tilde{y}_i = c \leftrightarrow y_i = c \wedge p(c|x_i) > \text{Max}\{p(c_n|x_i)|c_n \in D_{c-ns}\}. \quad (2)$$

4 LNL+K Baseline Methods

In this section, we present our baseline methods of adapting LNL methods to use noise source distribution knowledge. Our adaptations focus on methods that aim to detect clean samples. Once the samples are selected, the rest of the training remains the same as the original methods. This consists of a two-stage approach, where in the first warm-up stage the model trains with all the samples, and in the second stage, the model only trains using selected clean samples at each epoch. Fig. 2 provides an illustration of the baseline methods we use.

4.1 SFT^{+k}

SFT [22] detects noisy samples according to predictions stored in a memory bank \mathcal{M} . \mathcal{M} contains the last T epochs' predictions of each sample. A sample x_i is detected as noisy if a fluctuation event occurs, *i.e.*, the sample classified correctly at the previous epoch t_1 is misclassified at t_2 , where $t_1 < t_2$. The occurrence of the fluctuation event can be formulated as $fluctuation(x_i, y_i) = 1$, otherwise $fluctuation(x_i, y_i) = 0$ *i.e.*,

$$\begin{aligned} fluctuation(x_i, y_i) = 1 &\leftrightarrow \exists t_1, t_2 \in \{t - T, \dots, T\} \wedge t_1 < t_2 \\ &s.t. f_\theta(x_i)^{t_1} = y_i \wedge f_\theta(x_i)^{t_2} \neq y_i, \end{aligned} \quad (3)$$

where $f_\theta(x_i)^{t_1}$ represents the prediction of x_i at epoch t_1 . SFT is a probability-distribution-based approach and can fit our probabilistic model as follows. The propositional logic of SFT is,

$$p(c|x_i) = \begin{cases} 1 & : y_i = c \wedge fluctuation(x_i, y_i) = 0 \\ 0 & : otherwise. \end{cases} \quad (4)$$

I.e., SFT^{+k} applies the noise source distribution knowledge to SFT by relaxing the constraints of fluctuation. The fluctuation events only occur when the previous correct prediction is misclassified as the noise source label. For example, in Fig. 2, the noisy red triangle was classified correctly as "red" at epoch $t - 1$ but classified incorrectly as "yellow", which is the noise source class, at epoch t . Since a fluctuation event occurs, the red triangle is detected as noisy. Thus, we define SFT^{+k} fluctuation as,

$$\begin{aligned} fluctuation(x_i, y_i, D_{y_i-ns}) = 1 &\leftrightarrow \exists c_n \in D_{y_i-ns}, \exists t_1, t_2 \in \{t - T, \dots, T\} \wedge t_1 < t_2, \\ &s.t. f_\theta(x_i)^{t_1} = y_i \wedge f_\theta(x_i)^{t_2} = c_n. \end{aligned} \quad (5)$$

Combining Eq. 2, Eq. 4 and Eq. 5, SFT^{+k} detects x_i with clean label $y_i = \tilde{y}_i = c$ with $p(c|x_i)$ as:

$$\begin{aligned} \tilde{y}_i = c &\leftrightarrow y_i = c \wedge p(c|x_i) > \text{Max}(\{p(c_n|x_i)|c_n \in D_{c-ns}\}) \\ \leftrightarrow y_i = c \wedge p(c|x_i) = 1 &\leftrightarrow y_i = c \wedge fluctuation(x_i, y_i, D_{y_i-ns}) = 0. \end{aligned} \quad (6)$$

4.2 CRUST^{+k}

The key idea of CRUST [10] is from the neural network Jacobian matrix containing all its first-order partial derivatives. It is proved in their work that the neural network has a low-rank Jacobian matrix for clean samples. In other words, data points with clean labels in the same class often have similar gradients clustered closely together. CRUST is a feature-based method and this approach can be summarized with settings in Section 3.1. The feature used for selection is the pairwise gradient distance within the class: $g(X_c) = \{d_{x_i x_j}(\mathcal{W})|x_i, x_j \in X_c\}$, where $d_{x_i x_j}(\mathcal{W}) = \|\nabla L(\mathcal{W}, x_i) - \nabla L(\mathcal{W}, x_j)\|_2$, \mathcal{W} is the network parameters and $L(\mathcal{W}, x_i) = \frac{1}{2} \sum_{x_i \in D} (y_i - f_\theta(\mathcal{W}, x_i))^2$. CRUST needs an additional parameter β to control the size of the clean selection set X'_c . Given β , the sample x_i is selected as clean if $\|X'_c\| = \beta$ ($\|X'_c\|$ is the size of set X'_c) and $x_i \in X'_c$, where $\sum g(X'_c)$ has the minimum value. *i.e.*, the selected clean subset X'_c has the most similar gradients clustered together. Thus, we can summarize the similarity metric M for $p(c|x_i)$ as:

$$\begin{aligned} M(x_i, \phi_c, \beta) = 1 &\leftrightarrow \exists X'_c \subset X_c \wedge \|X'_c\| = \beta, \\ &s.t. x_i \in X'_c \wedge (\forall \|X''_c\| = \beta \wedge X''_c \subset X_c, \sum g(X'_c) \leq \sum g(X''_c)), \end{aligned} \quad (7)$$

otherwise $M(x_i, \phi_c, \beta) = 0$. Thus, we can get the propositional logic of CRUST:

$$\tilde{y}_i = c \leftrightarrow y_i = c \wedge p(c|x_i) = 1 \leftrightarrow M(x_i, \phi_{y_i}, \beta) = 1. \quad (8)$$

To adapt CRUST to CRUST^{+k} with noise source distribution knowledge. from Eq.2, we have

$$\begin{aligned} y_i = c \wedge \tilde{y}_i \neq c &\leftrightarrow p(c|x_i) \leq \text{Max}(\{p(c_n|x_i)|c_n \in D_{c-ns}\}) \\ \leftrightarrow \exists c_n \in D_{c-ns} s.t. p(c_n|x_i) \geq p(c|x_i) &\leftrightarrow \exists c_n \in D_{c-ns} s.t. p(c_n|x_i) = 1. \end{aligned} \quad (9)$$

To get $p(c_n|x_i)$, we first mix x_i with all the samples in X_{c_n} , *i.e.*, $X_{c_n+} = \{x_i\} \cup X_{c_n}$. Then apply CRUST on this mix set, *i.e.*, calculate the loss towards label c_n and select the clean subset X'_{c_n+} . if $x_i \in X'_{c_n+}$, then $p(c_n|x_i) = 1$. For example, in Fig. 2, to select clean-label samples in the red class, we first mix the red class with its noise source yellow class (If there are multiple

noise source classes, we repeat this process for each class), then we calculate the gradients with all yellow labels. If the sample’s true label is yellow, then the gradients should be similar to other yellow samples, which can be captured with CRUST on the entire mix set. The clean samples in red are those that don’t belong to the yellow class CRUST cluster. Here is the formulation of CRUST^{+k}, we modify $L(\mathcal{W}, x_i)$ to $L(\mathcal{W}, x_i, c) = \frac{1}{2} \sum_{x_i \in D} (c - f_\theta(\mathcal{W}, x_i))^2$, where we calculate the loss to any certain categories, not limited to the loss towards the label. Similarly, we have $d_{x_i x_j}(\mathbf{W}, c) = \|\nabla L(\mathcal{W}, x_i, c) - \nabla L(\mathcal{W}, x_j, c)\|_2$, $g(X_{c_n+}, c_n) = \{d_{x_i x_j}(\mathbf{W}, c_n) | x_i, x_j \in X_{c_n+}\}$. We use γ to represent the subset size of X_{c+c_n} , which is decided by β and noise source distribution. Finally, we get the similarity metric $M(x_i, \phi_{c_n+}, \gamma)$ as:

$$M(x_i, \phi_{c_n+}, \gamma) = 1 \leftrightarrow \exists X'_{c_n+} \subset X_{c_n+} \wedge \|X'_{c_n+}\| = \gamma, \quad (10)$$

$$s.t. x_i \in X'_{c_n+} \wedge (\forall \|X''_{c_n+}\| = \gamma \wedge X''_{c_n+} \subset X_{c_n+}, \sum g(X'_{c_n+}, c_n) \leq \sum g(X''_{c_n+}, c_n)),$$

otherwise $M(x_i, \phi_{c_n+}, \gamma) = 0$. Combining Eq.2, Eq.8, and Eq.10, $p(c|x_i)$ of CRUST^{+k} method is:

$$\begin{aligned} \tilde{y}_i = c &\leftrightarrow y_i = c \wedge (\forall c_n \in D_{c-ns}, p(c_n|x_i) < p(c|x_i)) \\ &\leftrightarrow y_i = c \wedge (\forall c_n \in D_{c-ns}, p(c_n|x_i) = 0) \leftrightarrow y_i = c \wedge (\forall c_n \in D_{c-ns}, M(x_i, \phi_{c_n+}, \gamma) = 0). \end{aligned} \quad (11)$$

4.3 FINE^{+k}

Filtering Noisy instances via their Eigenvectors(FINE) [9] selects clean samples with the feature-based method. Let $f_{\theta^*}(x_i)$ be the feature extractor output and Σ_c be the gram matrix of all features labeled as category c . The alignment is defined as the cosine distance between feature $\overrightarrow{f_{\theta^*}(x_i)}$ and \overrightarrow{c} , which is the eigenvector of the Σ_c and can be treated as the feature representation of category c . FINE fits a Gaussian Mixture Model (GMM) on the alignment distribution to divide samples to clean and noisy groups - the clean group has a larger mean value, which refers to a better alignment with the category feature representation. In summary, feature mapping function $g(x_i, c) = \langle \overrightarrow{f_{\theta^*}(x_i)}, \overrightarrow{c} \rangle$, and mixture of Gaussian distributions $\phi_c = \mathcal{N}_{clean} + \mathcal{N}_{noisy} = \mathcal{N}(\mu_{g(X_{c-clean})}, \sigma_{g(X_{c-clean})}) + \mathcal{N}(\mu_{g(X_{c-noisy})}, \sigma_{g(X_{c-noisy})})$, where $\mu_{g(X_{c-clean})} > \mu_{g(X_{c-noisy})}$. The similarity metric

$$M(x_i, \phi_c) = \begin{cases} 1 & : \mathcal{N}_{clean}(g(x_i, c)) > \mathcal{N}_{noisy}(g(x_i, c)) \\ 0 & : \mathcal{N}_{clean}(g(x_i, c)) \leq \mathcal{N}_{noisy}(g(x_i, c)). \end{cases} \quad (12)$$

Thus, we have

$$\tilde{y}_i = c \leftrightarrow y_i = c \wedge p(c|x_i) = 1 \leftrightarrow M(x_i, \phi_{y_i}) = 1. \quad (13)$$

Next, we show our design of FINE^{+k} with noise source distribution knowledge. The key difference between FINE and FINE^{+k} is that we use the alignment score of the noise source class. For example, in Fig. 2, the FINE^{+k} score is the difference between the red class alignment score and the yellow class alignment score, then we fit GMM on this FINE^{+k} score. Noisy samples in the red class would have better alignment with the yellow class eigenvector, thus a lower mean in the FINE^{+k} score distribution. For a formal description of FINE^{+k}, We define $g_k(x_i, c, c_n) = g(x_i, c) - g(x_i, c_n)$. Similar to FINE, FINE^{+k} fits a GMM on $g_k(X_c, c, c_n)$, so we have $g_k(X_c, c, c_n) \sim \phi_{k-\{c+c_n\}} = \mathcal{N}_{close-c} + \mathcal{N}_{close-c_n}$, where $\mu_{close-c} > \mu_{close-c_n}$. This can be interpreted in the following way: Samples aligning better with category c should have larger $g(x_i, c)$ values and smaller $g(x_i, c_n)$ values according to the assumption, thus the greater the $g_k(x_i, c, c_n)$, the closer to category c , vice versa, the smaller the $g_k(x_i, c, c_n)$, the closer to category c_n . Then we have

$$M(x_i, \phi_{k-\{c+c_n\}}) = \begin{cases} 1 & : \mathcal{N}_{close-c}(g_k(x_i, c, c_n)) > \mathcal{N}_{close-c_n}(g_k(x_i, c, c_n)) \\ 0 & : \mathcal{N}_{close-c}(g_k(x_i, c, c_n)) \leq \mathcal{N}_{close-c_n}(g_k(x_i, c, c_n)). \end{cases} \quad (14)$$

By combining with Eq.2, we have

$$\begin{aligned} \tilde{y}_i = c &\leftrightarrow y_i = c \wedge (\forall c_n \in D_{c-ns}, p(c|x_i) > p(c_n|x_i)) \\ &\leftrightarrow y_i = c \wedge (\forall c_n \in D_{c-ns}, M(x_i, \phi_{k-\{c+c_n\}}) = 1). \end{aligned} \quad (15)$$

5 Experiments

5.1 Datasets and Experiential Settings

CIFAR dataset with synthesized noise. CIFAR-10/CIFAR-100 [19] dataset contains 10/100 classes, with 5000/500 images per class for training and 1000/100 images per class for testing. We applied two synthesized noises with different noise ratios:

- **Asymmetric Noise** labels are generated by corrupting labels only to visually similar classes, *e.g.*, trucks \rightarrow automobiles, cat \rightarrow dog, horse \rightarrow deer. Experiments are over five noise ratios from 10% to 90%. For example, in the 90% noise ratio setting, 90% images in trucks, cat, and horse classes are mislabeled as their visual-similar classes.
- **Dominant Noise** is a novel setting that simulates high-noise ratios in real-world datasets. We label classes as either "dominant" or "recessive," where samples mislabeled as the "recessive" class are likely from the "dominant" class. In CIFAR-10/CIFAR-100 [19] dataset, we set half categories as different "recessive" classes and the other half categories are different "dominant" classes. Noisy labels are generated by labeling images in "dominant" as "recessive". In contrast to symmetric noise, where noisy samples are uniformly distributed across multiple classes, assuming the existence of "dominant" noise source class(es) is more plausible. In addition, the number of clean samples in a class with high symmetric noise is still significantly higher than the number of noisy samples from each class. For example, in the 50% symmetric noise ratio CIFAR-10 setting, where 50% of the noise is uniformly distributed across the other 9 classes, resulting in approximately 6% noise from each class, the number of clean samples in a class still surpasses the number of noisy samples by a factor of 10. While in dominant noise, 50% of the noise is only from the "dominant" class, thus, the class distribution is more likely to be skewed by the noisy labels. Note that this breaks the informative dataset assumption used by prior work [21].

Cell dataset BBBC036 with natural noise. Cell images for our experiments are from the Cell Painting [23] datasets, which represent large treatment screens of chemical and genetic perturbations. The BBBC036 dataset is high-throughput compound screens testing 1500 bioactive compounds (treatments). The dataset² was obtained by exposing U2OS cells (human bone osteosarcoma) to the treatments. Each treatment is tested in 5 replicates, using multi-well plates, and then imaged with the Cell Painting protocol [23], which is based on six fluorescent markers captured in five channels.

Our goal is to classify the effects of treatments with cell morphology features trained by the model. The challenge of this task is that cells have different degrees of reaction to the treatment, *i.e.*, some treatments are so weak that little difference can be recognized from control features. Thus, the noisy labels in this dataset are those cell images that look like controls (doing-nothing group) but are labeled as treatments. In fact, around 1300 of the 1500 treatments show high feature similarity with the control group. The true noise ratio is unknown and for those weak treatments, the majority of the cell images might all be noisy. We reconstruct the cell dataset with 15 weak treatments and 85 normal-reaction treatments and report results on this dataset.

Baselines. In addition to the methods we adapt, we also compare to Co-teaching[11], a loss-based sample selection method that trains a pair of networks, where each samples small-loss examples as useful training data for its peer network. For the synthesized data, we also show the results of the vanilla method and the oracle method. *i.e.*, Vanilla is training with all the samples (no clean sample selection), and Oracle is training with all the clean samples.

Metrics. Each dataset splits into training, validation, and test set, where training and validation contain noisy labels and the test is clean. For low-noise-ratio(lower than 0.5) and real noise settings, the model with the highest validation accuracy is saved to report the top-1 test accuracy. For high-noise-ratio settings, the model of the last epoch is saved for testing. Reported results are averages three runs, due to space constraints, we provide error bars in the supplementary.

5.2 Results

Asymmetric noise Table 1 summarizes the performances in asymmetric noise settings, which shows the advantage of LNL+K in visually similar noise cases. Our adaptation methods CRUST^{+k}, FINE^{+k} and SFT^{+k} consistently outperform the original methods in most noise settings. The advantages

²Available at https://bbbc.broadinstitute.org/image_sets

Table 1: Asymmetric noise results on CIFAR-10 and CIFAR-100 dataset. The best test accuracy is marked in bold, and the better result between LNL and LNL+K methods is marked with underlined. We find incorporating source knowledge helps in almost all cases. See Section 5.2 for discussion.

Noise ratio	CIFAR-10					CIFAR-100				
	0.1	0.3	0.5	0.7	0.9	0.1	0.3	0.5	0.7	0.9
Vanilla	93.54	91.85	84.21	69.86	67.70	62.06	61.43	59.26	57.23	56.36
Co-teaching [11]	93.04	89.86	63.66	44.46	19.26	69.26	69.56	60.99	54.07	37.81
CRUST [10]	93.08	89.59	83.95	81.11	75.18	62.81	62.59	57.69	58.16	53.55
CRUST ^{+k}	<u>93.46</u>	<u>92.79</u>	<u>89.45</u>	<u>83.11</u>	<u>81.56</u>	<u>63.79</u>	<u>64.12</u>	<u>62.96</u>	<u>63.20</u>	<u>58.57</u>
FINE [9]	89.54	88.43	88.03	87.13	76.67	57.49	56.45	57.25	51.92	49.90
FINE ^{+k}	<u>91.92</u>	<u>91.10</u>	<u>88.90</u>	87.62	83.53	61.70	62.47	63.04	60.55	60.31
SFT [22]	<u>92.96</u>	<u>91.68</u>	<u>86.27</u>	<u>67.17</u>	<u>67.01</u>	75.12	73.89	69.80	66.30	65.98
SFT ^{+k}	94.04	92.85	90.22	<u>85.10</u>	66.98	75.28	74.04	73.51	68.48	66.51
Oracle	94.26	94.2	93.58	92.51	88.98	63.50	64.75	61.77	62.61	59.73

Table 2: Dominant noise results on CIFAR-10 and CIFAR-100 dataset. The best test accuracy is marked in bold, and the better result between LNL and LNL+K methods is marked with underlined. We find incorporating source knowledge helps in almost all cases. See Section 5.2 for discussion.

Noise ratio	CIFAR-10			CIFAR-100		
	0.2	0.5	0.8	0.2	0.5	0.8
Vanilla	85.47	85.46	78.99	50.37	41.41	27.03
Co-teaching [11]	89.14	85.06	65.10	58.14	54.82	40.09
CRUST [10]	88.21	80.46	65.79	53.48	48.87	35.56
CRUST ^{+k}	<u>89.53</u>	<u>87.19</u>	80.54	58.69	<u>51.56</u>	<u>38.07</u>
FINE [9]	86.23	84.43	75.45	53.68	52.87	39.45
FINE ^{+k}	<u>88.69</u>	88.00	<u>80.52</u>	<u>57.22</u>	54.77	42.25
SFT [22]	89.48	85.43	75.43	51.82	48.21	<u>41.76</u>
SFT ^{+k}	89.78	<u>87.31</u>	<u>76.78</u>	<u>54.36</u>	<u>51.21</u>	37.96
Oracle	90.85	87.35	82.70	55.85	52.58	44.38

are particularly evident in high noise ratios where the LNL methods’ noise ratio upper bound is exceeded and the majority of samples in the noisy class have noisy labels. In the context of a 90% noise ratio on the CIFAR-100 dataset, the original LNL methods CRUST and FINE fail to outperform Vanilla’s performance. In contrast, our adaptation methods demonstrate comparable or even superior performance to the Oracle. Fig. 3 shows the embedding visualization of the four methods in a 90% asymmetric noise setting over CIFAR-10. We observe that the mislabeled confusing pairs are clustered together in the original methods, while are better separated in the adaptation methods.

Dominant noise Table 2 summarizes the performances in dominant noise settings, which shows the advantage of LNL+K moves beyond the noise ratio upper bound limit. Note that in the setting of 80% noise ratio over CIFAR-10 dataset, most methods can not even beat Vanilla’s performance, indicating that noisy samples strongly impact the class distribution, CRUST^{+k} and FINE^{+k} still perform better.

Natural noise The results for the noise in the cell dataset are shown in Table 3. Our adaptation methods have different degrees of improvement. The presence of high feature similarity between certain treatments and the "control" group can lead to significantly high noise ratios, ultimately strongly influencing the class distribution. This classification task is extremely challenging in that CRUST^{+k} is the only method that outperforms vanilla with 1.5% in top-1 accuracy.

5.3 Discussion: Knowledge Absorption and Future Directions

From the results in Section 5.2, we notice that the accuracy improvements of the adaptation methods vary in different noise settings and methods. We define knowledge absorption of method Q at task T

Table 3: BBBC036 cell data results. The best test accuracy is marked in bold, and the better result between LNL and LNL+K methods is marked with underlined. We find incorporating source knowledge helps in all cases. See Section 5.2 for discussion.

	Vanilla	CRUST [10]	CRUST ^{+k}	FINE [9]	FINE ^{+k}	SFT [22]	SFT ^{+k}
top 1	63.49	63.06	<u>65.07</u>	56.80	<u>57.01</u>	51.71	<u>59.18</u>
top 5	85.03	84.01	<u>85.06</u>	80.60	<u>81.28</u>	78.49	<u>81.58</u>

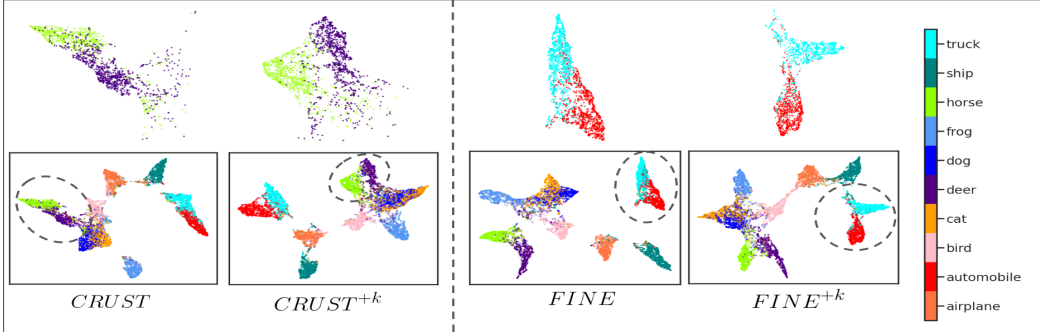


Figure 3: (Best view in color.) **Embedding visualization with UMAP.** 90% asymmetric noise over CIFAR-10 dataset. it is clear that our adaptation methods have better-separated clusters with confusing pairs (greenyellow: horse, indigo: deer) and (cyan: truck, red: automobile) .

as $KA(Q, T) = (A(Q^{+k}, T) - A(Q, T)) / A(Q, T)$, where $A(Q, T)$ is the accuracy of method Q at task T and $A(Q^{+k}, T)$ is the accuracy for adaptation method with knowledge.

Knowledge absorption varies for the same method at different noise settings. The key factors about the noise settings are noise ratio and the cleanness of the noise source. SFT^{+k} has higher KA with lower noise ratios in the synthesized noise settings. It is probably due to the fact that the frequency of "fluctuation" in SFT [22] is relevant to the noise ratio. It would be future work to analyze KA changes in different noise settings and what is the noise threshold for each adaptation method to achieve the maximum KA .

Knowledge absorption varies for different methods at the same noise settings. Considering the unified framework of detecting clean labels in Section 3, $p(c|x_i)$ and $p(c_n|x_i)$ are important factors to KA . SFT[22], CRUST[10], and FINE[9] represent three different methods of estimating $p(c|x_i)$. The results conclude that noise source knowledge might be more helpful to the feature-based clean sample detection methods in high noise ratios. KA indicates how well an LNL method can transfer to the LNL+K task with noise distribution knowledge, exploring ways to enhance the transferability of LNL methods and optimizing the value of KA are important areas for further investigation.

Limitations. Our assumption is that the knowledge of the noise source is available. Although one potentially find this automatically by using a confusion matrix, we leave exploring methods to automate this to future work. In addition, in our experiment settings, the "dominant" class is free of noise. Future work could also investigate the influence of the "dominant" class noise ratio to KA .

6 Conclusion

This paper introduces a new task, LNL+K, which leverages noise source distribution knowledge when learning with noisy labels. This knowledge is not only beneficial to distinguish clean samples that are ambiguous or out-of-distribution but also necessary when the noise ratio is so high that the noisy samples dominate the class distribution. Instead of comparing the "similarity" of the samples within the same class to detect the clean ones, LNL+K utilizes the "dissimilarity" between the sample and the noise source for detection. We provide a unified framework of clean sample detection for LNL+K which we use to adapt state-of-the-art LNL methods, CRUST^{+k}, FINE^{+k}, and SFT^{+k}, to our task. To create a more realistic simulation of high-noise-ratio settings, we introduce a novel noise setting called "dominant noise." Results show LNL+K methods have 5% average accuracy gains over asymmetric noise and up to 15% accuracy gains in the dominant noise setting. Finally, we discuss

"knowledge absorption", which notes the ranking of LNL methods to our task varies from their LNL performance, indicating that direct investigation of LNL+K is necessary.

Broader Impacts. The improved results on the cell dataset implies our work opens the door to LNL in scientific settings. At the same time, our work will have a social impact on domain experts, who can avoid some labor-intensive jobs such as correcting labels of medical images. However, we are also aware that LNL can enable bad actors to train a high-performing model as well.

References

- [1] Ranjay A Krishna, Kenji Hata, Stephanie Chen, Joshua Kravitz, David A Shamma, Li Fei-Fei, and Michael S Bernstein. Embracing error to enable rapid crowdsourcing. In *Proceedings of the 2016 CHI conference on human factors in computing systems*, pages 3167–3179, 2016.
- [2] Yan Yan, Rómer Rosales, Glenn Fung, Ramanathan Subramanian, and Jennifer Dy. Learning from multiple annotators with varying expertise. *Machine learning*, 95:291–327, 2014.
- [3] Nagarajan Natarajan, Inderjit S Dhillon, Pradeep K Ravikumar, and Ambuj Tewari. Learning with noisy labels. *Advances in neural information processing systems*, 26, 2013.
- [4] Devansh Arpit, Stanisław Jastrzębski, Nicolas Ballas, David Krueger, Emmanuel Bengio, Maxinder S Kanwal, Tegan Maharaj, Asja Fischer, Aaron Courville, Yoshua Bengio, et al. A closer look at memorization in deep networks. In *International conference on machine learning*, pages 233–242. PMLR, 2017.
- [5] Hwanjun Song, Minseok Kim, Dongmin Park, Yooju Shin, and Jae-Gil Lee. Learning from noisy labels with deep neural networks: A survey. *IEEE Transactions on Neural Networks and Learning Systems*, 2022.
- [6] Joshua Robinson, Ching-Yao Chuang, Suvrit Sra, and Stefanie Jegelka. Contrastive learning with hard negative samples. *arXiv preprint arXiv:2010.04592*, 2020.
- [7] Yannis Kalantidis, Mert Bulent Sariyildiz, Noe Pion, Philippe Weinzaepfel, and Diane Larlus. Hard negative mixing for contrastive learning. *Advances in Neural Information Processing Systems*, 33:21798–21809, 2020.
- [8] Zhi-Fan Wu, Tong Wei, Jianwen Jiang, Chaojie Mao, Mingqian Tang, and Yu-Feng Li. Ngc: A unified framework for learning with open-world noisy data. In *Proceedings of the IEEE/CVF International Conference on Computer Vision*, pages 62–71, 2021.
- [9] Taehyeon Kim, Jongwoo Ko, JinHwan Choi, Se-Young Yun, et al. Fine samples for learning with noisy labels. *Advances in Neural Information Processing Systems*, 34:24137–24149, 2021.
- [10] Baharan Mirzasoleiman, Kaidi Cao, and Jure Leskovec. Coresets for robust training of deep neural networks against noisy labels. *Advances in Neural Information Processing Systems*, 33:11465–11477, 2020.
- [11] Bo Han, Quanming Yao, Xingrui Yu, Gang Niu, Miao Xu, Weihua Hu, Ivor Tsang, and Masashi Sugiyama. Co-teaching: Robust training of deep neural networks with extremely noisy labels. *Advances in neural information processing systems*, 31, 2018.
- [12] Ahmet Iscen, Jack Valmadre, Anurag Arnab, and Cordelia Schmid. Learning with neighbor consistency for noisy labels. In *Proceedings of the IEEE/CVF Conference on Computer Vision and Pattern Recognition*, pages 4672–4681, 2022.
- [13] Ahmet Iscen, Giorgos Tolias, Yannis Avrithis, and Ondrej Chum. Label propagation for deep semi-supervised learning. In *Proceedings of the IEEE/CVF conference on computer vision and pattern recognition*, pages 5070–5079, 2019.
- [14] Dengyong Zhou, Olivier Bousquet, Thomas Lal, Jason Weston, and Bernhard Schölkopf. Learning with local and global consistency. *Advances in neural information processing systems*, 16, 2003.
- [15] Duc Tam Nguyen, Chaithanya Kumar Mummadi, Thi Phuong Nhung Ngo, Thi Hoai Phuong Nguyen, Laura Beggel, and Thomas Brox. Self: Learning to filter noisy labels with self-ensembling. *arXiv preprint arXiv:1910.01842*, 2019.
- [16] Jiangfan Han, Ping Luo, and Xiaogang Wang. Deep self-learning from noisy labels. In *Proceedings of the IEEE/CVF international conference on computer vision*, pages 5138–5147, 2019.

- [17] Ryutaro Tanno, Ardavan Saeedi, Swami Sankaranarayanan, Daniel C Alexander, and Nathan Silberman. Learning from noisy labels by regularized estimation of annotator confusion. In *Proceedings of the IEEE/CVF conference on computer vision and pattern recognition*, pages 11244–11253, 2019.
- [18] Takuhiro Kaneko, Yoshitaka Ushiku, and Tatsuya Harada. Label-noise robust generative adversarial networks. In *Proceedings of the IEEE/CVF Conference on Computer Vision and Pattern Recognition*, pages 2467–2476, 2019.
- [19] Alex Krizhevsky, Geoffrey Hinton, et al. Learning multiple layers of features from tiny images. 2009.
- [20] Wikipedia contributors. Treatment and control groups — Wikipedia, the free encyclopedia, 2022. URL https://en.wikipedia.org/w/index.php?title=Treatment_and_control_groups&oldid=1110767032. [Online; accessed 24-April-2023].
- [21] Hao Cheng, Zhaowei Zhu, Xingyu Li, Yifei Gong, Xing Sun, and Yang Liu. Learning with instance-dependent label noise: A sample sieve approach. *arXiv preprint arXiv:2010.02347*, 2020.
- [22] Qi Wei, Haoliang Sun, Xiankai Lu, and Yilong Yin. Self-filtering: A noise-aware sample selection for label noise with confidence penalization. In *Computer Vision—ECCV 2022: 17th European Conference, Tel Aviv, Israel, October 23–27, 2022, Proceedings, Part XXX*, pages 516–532. Springer, 2022.
- [23] Mark-Anthony Bray, Shantanu Singh, Han Han, Chadwick T Davis, Blake Borgeson, Cathy Hartland, Maria Kost-Alimova, Sigrun M Gustafsdottir, Christopher C Gibson, and Anne E Carpenter. Cell painting, a high-content image-based assay for morphological profiling using multiplexed fluorescent dyes. *Nature protocols*, 11(9):1757–1774, 2016.
- [24] Aditya Pratapa, Michael Doron, and Juan C Caicedo. Image-based cell phenotyping with deep learning. *Current Opinion in Chemical Biology*, 65:9–17, 2021.
- [25] Xiaobo Xia, Tongliang Liu, Bo Han, Chen Gong, Nannan Wang, Zongyuan Ge, and Yi Chang. Robust early-learning: Hindering the memorization of noisy labels. In *International conference on learning representations*, 2021.
- [26] David Krueger, Nicolas Ballas, Stanislaw Jastrzebski, Devansh Arpit, Maxinder S Kanwal, Tegan Maharaj, Emmanuel Bengio, Asja Fischer, and Aaron Courville. Deep nets don’t learn via memorization. In *International conference on learning representations*, 2017.
- [27] Chiyuan Zhang, Samy Bengio, Moritz Hardt, Michael C Mozer, and Yoram Singer. Identity crisis: Memorization and generalization under extreme overparameterization. *arXiv preprint arXiv:1902.04698*, 2019.
- [28] Lu Jiang, Zhengyuan Zhou, Thomas Leung, Li-Jia Li, and Li Fei-Fei. Mentornet: Learning data-driven curriculum for very deep neural networks on corrupted labels. In *International conference on machine learning*, pages 2304–2313. PMLR, 2018.
- [29] Junnan Li, Richard Socher, and Steven CH Hoi. Dividemix: Learning with noisy labels as semi-supervised learning. *arXiv preprint arXiv:2002.07394*, 2020.
- [30] Eric Arazo, Diego Ortego, Paul Albert, Noel O’Connor, and Kevin McGuinness. Unsupervised label noise modeling and loss correction. In *International conference on machine learning*, pages 312–321. PMLR, 2019.
- [31] Wei Hu, QiHao Zhao, Yangyu Huang, and Fan Zhang. P-diff: Learning classifier with noisy labels based on probability difference distributions. In *2020 25th International Conference on Pattern Recognition (ICPR)*, pages 1882–1889. IEEE, 2021.
- [32] Reihaneh Torkzadehmahani, Reza Nasirigerdeh, Daniel Rueckert, and Georgios Kaissis. Label noise-robust learning using a confidence-based sieving strategy. *arXiv preprint arXiv:2210.05330*, 2022.
- [33] Daiki Tanaka, Daiki Ikami, Toshihiko Yamasaki, and Kiyoharu Aizawa. Joint optimization framework for learning with noisy labels. In *Proceedings of the IEEE conference on computer vision and pattern recognition*, pages 5552–5560, 2018.
- [34] Shikun Li, Xiaobo Xia, Shiming Ge, and Tongliang Liu. Selective-supervised contrastive learning with noisy labels. In *Proceedings of the IEEE/CVF Conference on Computer Vision and Pattern Recognition*, pages 316–325, 2022.
- [35] Mingchen Li, Mahdi Soltanolkotabi, and Samet Oymak. Gradient descent with early stopping is provably robust to label noise for overparameterized neural networks. In *International conference on artificial intelligence and statistics*, pages 4313–4324. PMLR, 2020.

- [36] Quanming Yao, Hansi Yang, Bo Han, Gang Niu, and James Tin-Yau Kwok. Searching to exploit memorization effect in learning with noisy labels. In *International Conference on Machine Learning*, pages 10789–10798. PMLR, 2020.
- [37] Yingbin Bai, Erkun Yang, Bo Han, Yanhua Yang, Jiatong Li, Yinian Mao, Gang Niu, and Tongliang Liu. Understanding and improving early stopping for learning with noisy labels. *Advances in Neural Information Processing Systems*, 34:24392–24403, 2021.
- [38] Aritra Ghosh, Himanshu Kumar, and P Shanti Sastry. Robust loss functions under label noise for deep neural networks. In *Proceedings of the AAAI conference on artificial intelligence*, 2017.
- [39] Xingjun Ma, Hanxun Huang, Yisen Wang, Simone Romano, Sarah Erfani, and James Bailey. Normalized loss functions for deep learning with noisy labels. In *International conference on machine learning*, pages 6543–6553. PMLR, 2020.
- [40] Yilun Xu, Peng Cao, Yuqing Kong, and Yizhou Wang. L_{dmi}: A novel information-theoretic loss function for training deep nets robust to label noise. *Advances in neural information processing systems*, 32, 2019.
- [41] Zhilu Zhang and Mert Sabuncu. Generalized cross entropy loss for training deep neural networks with noisy labels. *Advances in neural information processing systems*, 31, 2018.
- [42] Sheng Liu, Jonathan Niles-Weed, Narges Razavian, and Carlos Fernandez-Granda. Early-learning regularization prevents memorization of noisy labels. *Advances in neural information processing systems*, 33: 20331–20342, 2020.
- [43] Xiaobo Xia, Tongliang Liu, Bo Han, Chen Gong, Nannan Wang, Zongyuan Ge, and Yi Chang. Robust early-learning: Hindering the memorization of noisy labels. In *International conference on learning representations*, 2021.
- [44] Wei Hu, Zhiyuan Li, and Dingli Yu. Simple and effective regularization methods for training on noisily labeled data with generalization guarantee. *arXiv preprint arXiv:1905.11368*, 2019.
- [45] Filipe R Cordeiro, Ragav Sachdeva, Vasileios Belagiannis, Ian Reid, and Gustavo Carneiro. Longremix: Robust learning with high confidence samples in a noisy label environment. *Pattern Recognition*, 133: 109013, 2023.
- [46] Yanyao Shen and Sujay Sanghavi. Learning with bad training data via iterative trimmed loss minimization. In *International Conference on Machine Learning*, pages 5739–5748. PMLR, 2019.
- [47] Pengxiang Wu, Songzhu Zheng, Mayank Goswami, Dimitris Metaxas, and Chao Chen. A topological filter for learning with label noise. *Advances in neural information processing systems*, 33:21382–21393, 2020.
- [48] Kaiming He, Xiangyu Zhang, Shaoqing Ren, and Jian Sun. Deep residual learning for image recognition. In *Proceedings of the IEEE conference on computer vision and pattern recognition*, pages 770–778, 2016.
- [49] Kaiming He, Xiangyu Zhang, Shaoqing Ren, and Jian Sun. Identity mappings in deep residual networks. In *Computer Vision—ECCV 2016: 14th European Conference, Amsterdam, The Netherlands, October 11–14, 2016, Proceedings, Part IV 14*, pages 630–645. Springer, 2016.
- [50] Mingxing Tan and Quoc Le. Efficientnet: Rethinking model scaling for convolutional neural networks. In *International conference on machine learning*, pages 6105–6114. PMLR, 2019.

A Implementation Details

A.1 Datasets

A.1.1 CIFAR dataset with synthesized noise

Asymmetric noise. Labels are corrupted to visually similar classes. Pair (C_1, C_2) represents the samples in class C_1 are possibly mislabeled as C_2 . Noise ratios in the experiments are only the noise ratio in class C_1 , *i.e.* not the overall noise ratio. Here are the class pairs of CIFAR-10 and CIFAR-100 for asymmetric noise. **CIFAR-10** (trucks, automobiles), (cat, dog), (horse, deer). **CIFAR-100** (beaver, otter), (aquarium fish, flatfish), (poppies, roses), (bottles, cans), (apples, pears), (chair, couch), (bee, beetle), (lion, tiger), (crab, spider), (rabbit, squirrel), (maple, oak), (bicycle, motorcycle).

Dominant noise There are "recessive" and "dominant" classes in dominant noise. For CIFAR-10, category index of the last 5 are "recessive" classes and the first five are "dominant" classes. In other

words, category index 6-10 samples might be mislabeled as label index 1-5. Different numbers of samples are mixed for different noise ratios so that the dataset is still balanced after mislabeling. Table 4 shows the number of samples per category for each noise ratio.

Table 4: Sample composition for CIFAR-10/CIFAR-100 dominant noise

CIFAR-10 Dominant Noise			
Noise ratio	0.2	0.5	0.8
Dominant class	2000	1250	500
Recessive class	3000	3750	4500
CIFAR-100 Dominant Noise			
Noise ratio	0.2	0.5	0.8
Dominant class	200	125	50
Recessive class	300	375	450

A.1.2 Cell dataset BBBC036

For our experiments we subsampled 100 treatments to evaluate natural noise. Table 5 shows the treatment list. ("NA" refers to the control group, *i.e.* no treatment group.)

A.2 Model

We used a pre-trained ResNet34 [48] on CIFAR-10/CIFAR-100 datasets for most approaches, except for Co-teaching, which uses a pre-activation ResNet18 [49] following the author’s implementation. For experiments on BBBC036 we used an Efficient B0 [50] for all methods. To support the 5 channel images, we replaced the first convolutional layer in the network to support the new image dimensions.

A.3 Hyperparameters

For a fair comparison, we use the same hyperparameter settings as in prior work [9, 10, 22] for CIFAR-10/CIFAR-100 datasets. Hyperparameters of the cell dataset BBBC036 were set via grid search using the validation set. All the experiments use the same batch size of 128. "fl-ratio" of CRUST and CRUST^{+k}, which controls the size of selected clean samples is set as the same as the noise ratio in synthesized noise and set as 0.6 in cell dataset BBBC036. All the other hyperparameters for each dataset are summarized in Table 6.

B Detailed Results

We report the standard deviation of the accuracy, clean sample selection ratio, and selected-clean-sample number in Table7-Table22. We notice that our adaptation methods not only have higher average accuracy but also have higher clean ratios with a significantly larger number of clean samples.

C Analysis of Knowledge with Non-noise-source Classes

Noise source distribution knowledge not only helps classify classes with corrupted labels but is also beneficial to non-noise-source classes. Consider a non-noise-source class sample on the decision boundary, without knowledge, this sample is likely detected as noise and removed from training. Fig. 4 demonstrates this point. Asymmetric noise pairs are not included as confusing pairs in the figure, *i.e.*, this figure only shows the confusing pairs between classes and their non-noise-source classes. Even those class objects are not visually similar, similar backgrounds can also lead to confusion, see Fig. 5 for examples. There are significantly large numbers of confusing pairs between "frog" and "bird" in the CRUST classifier compared with CRUST^{+k}. Furthermore, CRUST exhibits ambiguity between 'deer' and 'bird,' whereas such ambiguity is less prominent or observable in CRUST^{+k}. One explanation is that "bird" is not in the noise source of "deer", thus bird samples on the decision boundary will be selected as clean samples. Training with these clean hard negatives helps the model better classify the confusing samples.

Table 5: Treatments used from the BBBC036 dataset

Weak-reaction Treatments				
NA	BRD-K88090157	BRD-K38436528	BRD-K07691486	BRD-K97530723
BRD-A32505112	BRD-K21853356	BRD-K96809896	BRD-A82590476	BRD-A95939040
BRD-A53952395	BRD-A64125466	BRD-A99177642	BRD-K90574421	BRD-K07507905
Normal-reaction Treatments				
BRD-K62221994	BRD-K62810658	BRD-K47150025	BRD-K17705806	BRD-K85015012
BRD-K37865504	BRD-A52660433	BRD-K66898851	BRD-K15025317	BRD-K37392901
BRD-K91370081	BRD-K39484304	BRD-K03842655	BRD-K76840893	BRD-K62289640
BRD-K14618467	BRD-K52313696	BRD-K43744935	BRD-K86727142	BRD-K21680192
BRD-K06426971	BRD-K24132293	BRD-K68143200	BRD-K08554278	BRD-K78122587
BRD-A47513740	BRD-K18619710	BRD-A67552019	BRD-K17140735	BRD-K30867024
BRD-K36007650	BRD-K51318897	BRD-K90382497	BRD-K00259736	BRD-K95435023
BRD-K52075040	BRD-K03642198	BRD-K47278471	BRD-K17896185	BRD-K95603879
BRD-A70649075	BRD-K02407574	BRD-A90462498	BRD-K67860401	BRD-A64485570
BRD-K88429204	BRD-A49046702	BRD-K50841342	BRD-K35960502	BRD-K77171813
BRD-K54095730	BRD-K93754473	BRD-K22134346	BRD-K72703948	BRD-K31342827
BRD-K31542390	BRD-K18250272	BRD-K00141480	BRD-K37991163	BRD-K13533483
BRD-K67439147	BRD-A91008255	BRD-K39187410	BRD-K26997899	BRD-K89732114
BRD-K50135270	BRD-K95237249	BRD-K44849676	BRD-K20742498	BRD-K31912990
BRD-K96799727	BRD-K09255212	BRD-A89947015	BRD-K78364995	BRD-K49294207
BRD-K08316444	BRD-K89930444	BRD-K50398167	BRD-K47936004	BRD-A72711497
BRD-A97104540	BRD-A50737080	BRD-K80970344	BRD-K50464341	BRD-K97399794

Table 6: Hyperparameters for each dataset.

	learning rate	warm-up epochs	total epochs
CIFAR-10/CIFAR-100	1e-2	40	120
BBBC036	1e-1	10	50

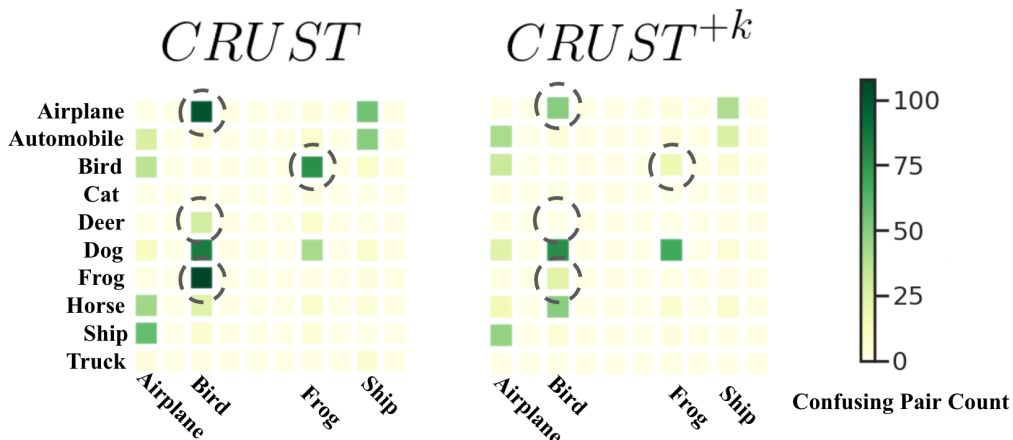


Figure 4: (Best view in color.) **Non-noise-source confusing pairs visualization.** 90% asymmetric noise over CIFAR-10 dataset. Confusing pair counts visualization. (The column has the same index as the row from left to right.) Confusing pair (i, j) refers to the sample from category j being misclassified as i or lying on the decision boundary between i and j . It is clear that our adaptation methods have fewer confusing pairs. See Section C for discussion.

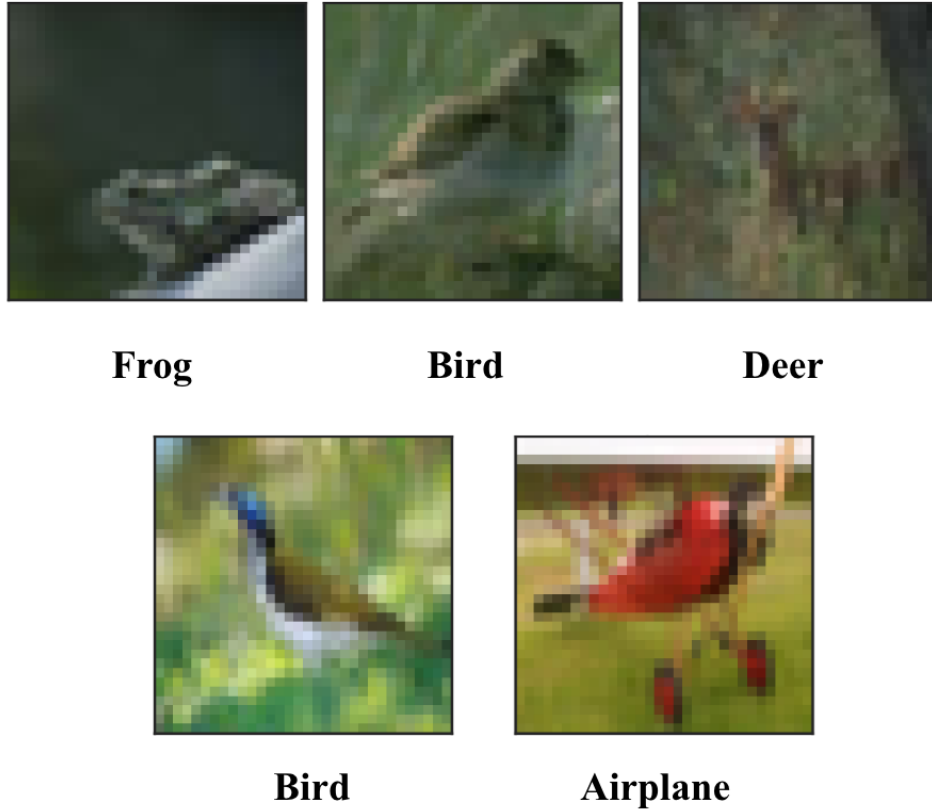


Figure 5: (Best view in color.) **Non-noise-source confusing image samples of CIFAR-10 dataset.** Sample images from CIFAR-10 dataset that are easily confused with each other. See Section C for discussion.

Table 7: Asymmetric noise (ratio 0.1) results on CIFAR-10 dataset. The best test accuracy is marked in bold, and the better result between LNL and LNL+K methods is marked with underlined.

CIFAR-10 Aymmetric Noise 0.1										
	Accuracy			AVG-Acc	STD-Acc	Clean Ratio			AVG-Ratio	Clean Sample
Vanilla	93.71	93.61	93.30	93.72	0.21	97.00	97.00	97.00	97.00	43650
Co-teaching [11]	93.16	92.99	92.97	93.04	0.10	99.62	99.62	99.62	99.62	40626
CRUST [10]	93.10	93.03	93.11	93.18	0.04	99.54	99.55	99.55	<u>99.55</u>	40317
CRUST ^{+k}	93.50	93.40	93.48	<u>93.46</u>	0.05	97.09	96.99	96.96	97.01	<u>42209</u>
FINE [9]	89.79	89.42	89.41	89.54	0.22	99.95	99.95	99.95	99.95	29615
FINE ^{+k}	92.02	91.83	91.91	<u>91.92</u>	0.10	99.96	99.96	99.96	99.96	<u>37039</u>
SFT [22]	93.06	92.93	92.89	92.96	0.09	99.46	99.43	99.46	99.45	43071
SFT ^{+k}	94.01	94.07	94.04	94.04	0.03	99.79	99.79	99.79	<u>99.79</u>	43330
Oracle	94.41	94.20	94.17	94.26	0.13	100.00	100.00	100.00	100.00	43650

Table 8: Asymmetric noise (ratio 0.3) results on CIFAR-10 dataset. The best test accuracy is marked in bold, and the better result between LNL and LNL+K methods is marked with underlined.

CIFAR-10 Asymmetric Noise 0.3										
	Accuracy			AVG-Acc	STD-Acc	Clean Ratio			AVG-Ratio	Clean Sample
Vanilla	92.04	91.77	91.74	91.85	0.17	91.00	91.00	91.00	91.00	40950
Co-teaching [11]	89.67	89.81	90.10	89.86	0.22	99.31	99.38	99.41	99.36	32491
CRUST [10]	89.54	89.83	89.40	89.59	0.22	99.14	99.15	99.13	<u>99.14</u>	31229
CRUST ^{+k}	92.48	92.54	93.35	<u>92.79</u>	0.49	90.79	90.87	90.87	<u>90.84</u>	<u>36106</u>
FINE [9]	88.28	88.50	88.51	88.43	0.13	99.72	99.72	99.72	99.72	27446
FINE ^{+k}	90.91	91.11	91.28	<u>91.10</u>	0.19	99.67	99.67	99.67	99.67	<u>35584</u>
SFT [22]	91.85	91.69	91.50	91.68	0.18	97.40	97.39	97.39	97.40	40320
SFT ^{+k}	92.84	92.91	92.80	92.85	0.06	99.02	99.04	99.01	<u>99.03</u>	40659
Oracle	94.25	94.19	94.16	94.20	0.05	100.00	100.00	100.00	100.00	40950

Table 9: Asymmetric noise (ratio 0.5) results on CIFAR-10 dataset. The best test accuracy is marked in bold, and the better result between LNL and LNL+K methods is marked with underlined.

CIFAR-10 Asymmetric Noise 0.5										
	Accuracy			AVG-Acc	STD-Acc	Clean Ratio			AVG-Ratio	Clean Sample
Vanilla	84.36	84.33	83.94	84.21	0.23	85.00	85.00	85.00	85.00	38250
Co-teaching [11]	63.42	63.96	63.60	63.66	0.27	83.94	84.11	84.18	84.08	20657
CRUST [10]	83.88	83.56	84.41	83.95	0.43	97.90	97.90	97.85	<u>97.88</u>	22028
CRUST ^{+k}	89.36	89.40	89.59	<u>89.45</u>	0.12	85.85	86.04	86.07	85.98	<u>29939</u>
FINE [9]	87.88	87.93	88.28	<u>88.03</u>	0.22	99.69	99.69	99.69	99.69	<u>25386</u>
FINE ^{+k}	88.48	88.87	89.35	<u>88.90</u>	0.44	99.40	99.40	99.40	99.40	<u>33792</u>
SFT [22]	86.44	86.07	86.30	86.27	0.19	91.27	91.60	91.50	91.46	38003
SFT ^{+k}	90.11	89.71	90.84	90.22	0.57	96.04	95.53	95.92	<u>95.97</u>	37928
Oracle	93.55	93.58	93.61	93.58	0.03	100.00	100.00	100.00	100.00	38250

Table 10: Asymmetric noise (ratio 0.7) results on CIFAR-10 dataset. The best test accuracy is marked in bold, and the better result between LNL and LNL+K methods is marked with underlined.

CIFAR-10 Asymmetric Noise 0.7										
	Accuracy			AVG-Acc	STD-Acc	Clean Ratio			AVG-Ratio	Clean Sample
Vanilla	70.11	70.13	69.34	69.86	0.45	79.00	79.00	79.00	79.00	35550
Co-teaching [11]	44.98	44.86	43.54	44.46	0.80	77.45	77.67	76.62	77.24	12797
CRUST [10]	80.85	81.10	81.38	81.11	0.27	91.39	91.73	91.73	<u>91.61</u>	12338
CRUST ^{+k}	82.30	83.10	83.93	<u>83.11</u>	0.82	86.08	86.08	86.10	86.09	<u>24907</u>
FINE [9]	87.18	86.91	87.30	87.13	0.20	99.35	99.43	99.38	99.39	23731
FINE ^{+k}	87.61	87.46	87.79	87.62	0.17	97.83	97.83	97.89	97.85	<u>32301</u>
SFT [22]	67.17	67.16	67.18	67.17	0.01	76.87	76.94	76.93	76.91	31039
SFT ^{+k}	84.67	84.14	86.49	<u>85.10</u>	1.23	91.09	90.26	89.66	<u>90.34</u>	34135
Oracle	92.44	92.45	92.64	92.51	0.11	100.00	100.00	100.00	100.00	35550

Table 11: Asymmetric noise (ratio 0.9) results on CIFAR-10 dataset. The best test accuracy is marked in bold, and the better result between LNL and LNL+K methods is marked with underlined.

CIFAR-10 Asymmetric Noise 0.9										
	Accuracy			AVG-Acc	STD-Acc	Clean Ratio			AVG-Ratio	Clean Sample
Vanilla	67.68	67.91	67.51	67.70	0.20	73.00	73.00	73.00	73.00	32850
Co-teaching [11]	19.31	19.34	19.13	19.26	0.11	55.07	56.80	55.53	55.80	4646
CRUST [10]	75.18	74.99	75.37	75.18	0.19	76.18	76.07	76.18	76.14	3428
CRUST ^{+k}	81.54	81.52	81.62	<u>81.56</u>	0.05	93.11	93.05	93.11	<u>93.09</u>	<u>20404</u>
FINE [9]	76.67	75.08	78.26	76.67	1.59	90.43	90.43	90.43	90.43	22426
FINE ^{+k}	83.42	83.08	84.09	83.53	0.51	94.10	94.10	94.10	94.10	<u>30403</u>
SFT [22]	66.96	66.91	67.16	<u>67.01</u>	0.13	72.15	72.13	72.13	72.13	31371
SFT ^{+k}	66.95	66.99	67.00	66.98	0.02	73.06	73.06	73.05	<u>73.06</u>	32802
Oracle	88.75	88.35	89.84	88.98	0.77	100.00	100.00	100.00	100.00	32850

Table 12: Asymmetric noise (ratio 0.1) results on CIFAR-100 dataset. The best test accuracy is marked in bold, and the better result between LNL and LNL+K methods is marked with underlined.

CIFAR-100 Asymmetric Noise 0.1										
	Accuracy			AVG-Acc	STD-Acc	Clean Ratio			AVG-Ratio	Clean Sample
Vanilla	62.80	62.31	61.07	62.06	0.89	98.80	98.80	98.80	98.80	44460
Co-teaching [11]	69.47	69.21	69.10	69.26	0.19	99.28	99.26	99.25	99.27	40481
CRUST [10]	62.17	62.83	63.43	62.81	0.63	99.18	99.22	99.23	<u>99.21</u>	40158
CRUST ^{+k}	63.40	65.54	64.43	<u>63.79</u>	0.56	98.99	99.09	99.06	99.05	<u>43955</u>
FINE [9]	58.43	57.39	56.65	57.49	0.89	99.91	99.91	99.91	99.91	19337
FINE ^{+k}	60.64	61.53	62.93	<u>61.70</u>	1.15	99.89	99.89	99.89	99.89	<u>39972</u>
SFT [22]	75.21	75.08	75.07	<u>75.12</u>	0.08	99.66	99.66	99.66	99.66	41782
SFT ^{+k}	75.34	75.28	75.22	75.28	0.06	99.88	99.88	99.88	<u>99.88</u>	44029
Oracle	63.57	62.50	64.43	63.50	0.97	100.00	100.00	100.00	100.00	44460

Table 13: Asymmetric noise (ratio 0.3) results on CIFAR-100 dataset. The best test accuracy is marked in bold, and the better result between LNL and LNL+K methods is marked with underlined.

CIFAR-100 Asymmetric Noise 0.3										
	Accuracy			AVG-Acc	STD-Acc	Clean Ratio			AVG-Ratio	Clean Sample
Vanilla	61.63	61.74	60.92	61.43	0.45	96.40	96.40	96.40	96.40	43380
Co-teaching [11]	69.37	69.21	70.10	69.56	0.47	98.99	98.95	99.08	99.01	32346
CRUST [10]	60.93	63.18	63.66	62.59	1.46	98.44	98.52	98.63	<u>98.53</u>	31057
CRUST ^{+k}	63.83	65.54	62.99	<u>64.12</u>	1.30	97.60	97.49	97.42	97.50	<u>42019</u>
FINE [9]	56.67	56.87	55.81	56.45	0.56	99.46	99.46	99.46	99.46	19241
FINE ^{+k}	61.65	62.69	63.07	<u>62.47</u>	0.74	99.56	99.56	99.56	99.56	<u>40133</u>
SFT [22]	73.76	74.24	73.67	73.89	0.31	98.34	98.37	98.33	98.35	41269
SFT ^{+k}	74.21	73.78	74.13	74.04	0.23	99.39	99.39	99.39	<u>99.39</u>	43011
Oracle	64.39	64.65	65.21	64.75	0.42	100.00	100.00	100.00	100.00	43380

Table 14: Asymmetric noise (ratio 0.5) results on CIFAR-100 dataset. The best test accuracy is marked in bold, and the better result between LNL and LNL+K methods is marked with underlined.

CIFAR-100 Asymmetric Noise 0.5										
	Accuracy			AVG-Acc	STD-Acc	Clean Ratio			AVG-Ratio	Clean Sample
Vanilla	61.21	59.04	57.53	59.26	1.85	94.00	94.00	94.00	94.00	42300
Co-teaching [11]	61.17	61.12	60.68	60.99	0.27	94.38	94.38	94.35	94.37	23218
CRUST [10]	57.59	59.66	55.82	57.69	1.92	97.62	97.67	97.61	<u>97.63</u>	21950
CRUST ^{+k}	62.60	61.80	64.48	<u>62.96</u>	1.38	96.82	96.96	97.23	97.00	<u>39716</u>
FINE [9]	57.25	57.14	57.36	57.25	0.11	95.96	95.96	95.96	95.96	18984
FINE ^{+k}	62.47	63.02	63.63	<u>63.04</u>	0.58	98.96	98.98	98.96	98.97	<u>39738</u>
SFT [22]	69.47	69.44	70.49	<u>69.80</u>	0.60	94.19	94.20	94.19	<u>94.20</u>	39316
SFT ^{+k}	73.42	73.44	73.67	73.51	0.14	97.97	97.96	97.94	<u>97.96</u>	42014
Oracle	62.03	62.07	61.21	61.77	0.49	100.00	100.00	100.00	100.00	42300

Table 15: Asymmetric noise (ratio 0.7) results on CIFAR-100 dataset. The best test accuracy is marked in bold, and the better result between LNL and LNL+K methods is marked with underlined.

CIFAR-100 Asymmetric Noise 0.7										
	Accuracy			AVG-Acc	STD-Acc	Clean Ratio			AVG-Ratio	Clean Sample
Vanilla	57.22	57.51	56.96	57.23	0.28	91.60	91.60	91.60	91.60	41220
Co-teaching [11]	53.84	54.07	54.30	54.07	0.23	89.73	90.03	89.94	89.90	14854
CRUST [10]	58.02	58.12	58.34	58.16	0.16	93.86	93.76	93.79	93.80	12651
CRUST ^{+k}	63.20	62.22	64.18	<u>63.20</u>	0.98	97.29	97.18	97.36	97.28	<u>37457</u>
FINE [9]	51.91	51.26	52.59	51.92	0.67	90.42	90.42	90.42	90.42	18545
FINE ^{+k}	61.49	60.50	59.66	<u>60.55</u>	0.92	98.34	98.34	98.34	<u>98.34</u>	<u>39047</u>
SFT [22]	66.40	65.30	66.20	<u>66.30</u>	0.10	91.11	91.11	91.11	91.11	37848
SFT ^{+k}	68.63	68.66	68.15	68.48	0.29	92.83	92.80	92.82	<u>92.82</u>	40982
Oracle	62.28	62.53	63.02	62.61	0.38	100.00	100.00	100.00	100.00	41220

Table 16: Asymmetric noise (ratio 0.9) results on CIFAR-100 dataset. The best test accuracy is marked in bold, and the better result between LNL and LNL+K methods is marked with underlined.

CIFAR-100 Asymmetric Noise 0.9										
	Accuracy			AVG-Acc	STD-Acc	Clean Ratio			AVG-Ratio	Clean Sample
Vanilla	56.24	56.36	56.48	56.36	0.12	89.20	89.20	89.20	89.20	40140
Co-teaching [11]	37.80	35.79	39.84	37.81	2.03	83.96	83.83	84.14	83.98	7084
CRUST [10]	53.55	54.34	52.76	53.55	0.79	86.85	87.03	86.52	86.80	3898
CRUST ^{+k}	57.73	60.34	57.64	<u>58.57</u>	1.53	98.68	98.81	98.89	98.80	<u>35357</u>
FINE [9]	48.76	51.07	49.87	49.90	1.16	86.84	86.84	86.84	86.84	17813
FINE ^{+k}	59.43	59.66	61.84	<u>60.31</u>	1.33	96.98	96.98	97.23	<u>97.06</u>	<u>38885</u>
SFT [22]	65.93	65.98	66.03	65.98	0.05	88.83	88.83	88.82	88.82	37877
SFT ^{+k}	66.94	67.09	65.5	66.51	0.88	89.37	89.38	89.37	<u>89.37</u>	39959
Oracle	59.73	59.73	59.73	59.73	0.00	100.00	100.00	100.00	100.00	40140

Table 17: Dominant noise (ratio 0.2) results on CIFAR-10 dataset. The best test accuracy is marked in bold, and the better result between LNL and LNL+K methods is marked with underlined.

CIFAR-10 Dominant Noise 0.2										
	Accuracy			AVG-Acc	STD-Acc	Clean Ratio			AVG-Ratio	Clean Sample
Vanilla	85.23	85.11	86.07	85.47	0.52	90.00	90.00	90.00	90.00	20250
Co-teaching [11]	89.10	89.05	89.27	89.14	0.12	99.39	99.37	99.43	99.39	18174
CRUST [10]	88.12	88.05	88.46	88.21	0.22	98.71	98.66	98.70	<u>98.69</u>	17761
CRUST ^{+k}	89.52	89.49	89.58	<u>89.53</u>	0.05	97.78	97.97	97.82	97.85	<u>19856</u>
FINE [9]	86.10	86.02	86.57	86.23	0.30	99.90	99.90	99.90	99.90	13279
FINE ^{+k}	88.76	88.64	88.67	<u>88.69</u>	0.06	99.92	99.92	99.92	99.92	<u>18148</u>
SFT [22]	89.38	89.72	89.34	89.48	0.21	98.68	98.68	98.75	98.70	19806
SFT ^{+k}	89.76	89.76	89.82	89.78	0.03	99.46	99.48	98.75	<u>99.23</u>	19983
Oracle	90.75	90.87	90.93	90.85	0.09	100.00	100.00	100.00	100.00	20250

Table 18: Dominant noise (ratio 0.5) results on CIFAR-10 dataset. The best test accuracy is marked in bold, and the better result between LNL and LNL+K methods is marked with underlined.

CIFAR-10 Dominant Noise 0.5										
	Accuracy			AVG-Acc	STD-Acc	Clean Ratio			AVG-Ratio	Clean Sample
Vanilla	85.38	85.26	85.74	85.46	0.25	75.00	75.00	75.00	75.00	16875
Co-teaching [11]	84.98	85.25	84.95	85.06	0.17	99.75	99.74	99.76	99.75	12270
CRUST [10]	80.33	80.40	80.65	80.46	0.17	95.71	95.51	95.64	95.62	10758
CRUST ^{+k}	87.17	87.28	87.12	<u>87.19</u>	0.08	95.79	95.61	95.72	<u>95.71</u>	<u>16596</u>
FINE [9]	84.16	84.87	84.26	<u>84.43</u>	0.38	98.93	98.93	98.93	<u>98.93</u>	11416
FINE ^{+k}	87.91	87.97	88.12	88.00	0.11	96.88	96.88	96.88	96.88	16750
SFT [22]	85.34	85.37	85.58	85.43	0.13	93.52	93.50	93.65	93.56	15038
SFT ^{+k}	87.21	87.48	87.24	<u>87.31</u>	0.15	97.85	97.80	97.82	<u>97.82</u>	<u>16006</u>
Oracle	87.31	87.28	87.46	87.35	0.10	100.00	100.00	100.00	100.00	16875

Table 19: Dominant noise (ratio 0.8) results on CIFAR-10 dataset. The best test accuracy is marked in bold, and the better result between LNL and LNL+K methods is marked with underlined.

CIFAR-10 Dominant Noise 0.8										
	Accuracy			AVG-Acc	STD-Acc	Clean Ratio			AVG-Ratio	Clean Sample
Vanilla	78.91	79.01	79.05	78.99	0.07	60.00	60.00	60.00	60.00	13500
Co-teaching [11]	64.81	64.51	65.98	65.10	0.78	93.73	91.86	93.89	93.16	12053
CRUST [10]	65.54	65.33	66.50	65.79	0.62	72.43	71.81	72.62	72.29	4880
CRUST ^{+k}	80.29	80.46	80.87	80.54	0.30	87.60	87.86	87.53	<u>87.67</u>	<u>13370</u>
FINE [9]	74.92	75.13	76.30	75.45	0.74	88.53	88.53	88.53	88.53	8355
FINE ^{+k}	80.27	80.47	80.82	<u>80.52</u>	0.28	89.64	89.64	89.64	<u>89.64</u>	13448
SFT [22]	75.31	75.44	75.54	75.43	0.12	97.28	97.25	97.28	97.27	12740
SFT ^{+k}	76.77	76.41	77.16	<u>76.78</u>	0.38	98.97	99.00	99.00	98.99	<u>12818</u>
Oracle	82.63	83.11	82.36	82.70	0.38	100.00	100.00	100.00	100.00	13500

Table 20: Dominant noise (ratio 0.2) results on CIFAR-100 dataset. The best test accuracy is marked in bold, and the better result between LNL and LNL+K methods is marked with underlined.

CIFAR-100 Dominant Noise 0.2										
	Accuracy			AVG-Acc	STD-Acc	Clean Ratio			AVG-Ratio	Clean Sample
Vanilla	49.92	50.37	50.82	50.37	0.45	90.00	90.00	90.00	90.00	20250
Co-teaching [11]	58.00	57.96	58.46	58.14	0.28	98.08	98.12	98.14	98.11	17942
CRUST [10]	52.97	53.07	54.40	53.48	0.80	96.90	96.87	96.96	<u>96.91</u>	17400
CRUST ^{+k}	58.58	58.25	59.24	58.69	0.50	94.87	94.80	94.82	94.83	<u>18500</u>
FINE [9]	53.05	52.55	55.44	53.68	1.54	99.49	99.49	99.49	99.49	12164
FINE ^{+k}	58.56	56.60	56.50	<u>57.22</u>	1.16	99.34	99.34	99.34	99.34	<u>18850</u>
SFT [22]	51.06	52.30	52.10	51.82	0.67	94.31	94.32	94.32	94.32	20068
SFT ^{+k}	54.16	54.01	54.91	<u>54.36</u>	0.48	97.54	97.54	97.55	<u>97.54</u>	19901
Oracle	55.92	55.11	56.52	55.85	0.71	100.00	100.00	100.00	100.00	20250

Table 21: Dominant noise (ratio 0.5) results on CIFAR-100 dataset. The best test accuracy is marked in bold, and the better result between LNL and LNL+K methods is marked with underlined.

CIFAR-100 Dominant Noise 0.5										
	Accuracy			AVG-Acc	STD-Acc	Clean Ratio			AVG-Ratio	Clean Sample
Vanilla	40.89	40.27	43.07	41.41	1.47	75.06	75.06	75.06	75.06	16850
Co-teaching [11]	54.63	54.62	55.21	54.82	0.34	98.16	98.18	98.56	98.30	12050
CRUST [10]	48.76	48.63	49.22	48.87	0.31	92.39	92.30	92.70	<u>92.46</u>	10355
CRUST ^{+k}	51.89	51.52	51.27	<u>51.56</u>	0.31	87.10	87.37	86.58	87.02	<u>16093</u>
FINE [9]	52.13	52.50	53.98	<u>52.87</u>	0.98	95.82	95.82	95.82	95.82	10574
FINE ^{+k}	53.55	54.07	56.69	<u>54.77</u>	1.68	97.87	97.87	97.87	<u>97.87</u>	<u>15966</u>
SFT [22]	47.65	49.60	47.38	48.21	1.21	86.06	86.10	86.05	86.07	16632
SFT ^{+k}	50.53	50.57	52.53	<u>51.21</u>	1.14	92.91	92.91	92.91	<u>92.91</u>	16511
Oracle	52.59	51.51	53.64	52.58	1.07	100.00	100.00	100.00	100.00	16850

Table 22: Dominant noise (ratio 0.8) results on CIFAR-100 dataset. The best test accuracy is marked in bold, and the better result between LNL and LNL+K methods is marked with underlined.

CIFAR-100 Dominant Noise 0.8										
	Accuracy			AVG-Acc	STD-Acc	Clean Ratio			AVG-Ratio	Clean Sample
Vanilla	27.17	26.94	26.98	27.03	0.12	60.00	60.00	60.00	60.00	13500
Co-teaching [11]	40.12	40.02	40.13	40.09	0.06	99.74	99.69	99.67	99.70	6138
CRUST [10]	33.99	36.60	36.09	35.56	1.38	64.64	65.63	64.62	64.96	2895
CRUST ^{+k}	36.02	38.08	40.11	<u>38.07</u>	2.05	85.10	84.48	84.48	<u>84.69</u>	<u>12769</u>
FINE [9]	39.51	39.18	39.66	39.45	0.25	77.70	77.70	77.70	77.70	8478
FINE ^{+k}	42.49	41.95	42.31	42.25	0.27	86.25	86.25	86.25	<u>86.25</u>	13249
SFT [22]	40.21	42.54	42.53	<u>41.76</u>	1.34	99.16	99.15	99.26	99.19	<u>11671</u>
SFT ^{+k}	37.92	37.95	38.01	37.96	0.05	99.96	99.96	99.96	99.96	11424
Oracle	44.36	44.56	44.22	44.38	0.17	100.00	100.00	100.00	100.00	13500